

# 1. INTRODUCTION

## 1.1 General:

One of the major concerns of process engineers, designers, and operators while dealing with heat exchangers is the vibration due to shell-side fluid flow across the tube bundles. Tubes vibrate when subjected to cross-flow of fluid and these vibrations are proportional to the velocity of fluid. These vibrations produce motion of higher amplitudes causing the premature tube failure in different forms like tube fretting, fatigue and wear. Many utility industries have lost millions of dollars due to the failure of handling this vibration problem.

The shutdown of different plants as a result of these vibrations motivated the researchers to examine this phenomenon caused by the fluid flow. Flow-induced vibration (FIV) can be characterized by five different excitation mechanisms including fluid elastic instability (FEI), vortex shedding, turbulent buffeting, jet switching and acoustic resonance. Turbulent buffeting and vortex shedding may cause a slight damage in tube bundles due to flow-induced vibrations over an extended amount of time or they generate high levels of noise due to acoustic resonance. These phenomena do not cause the tube failure, but it happens due to fluid elastic instability. Fluid elastic instability (FEI) occurs when the free-stream velocity in a cross flow tube bundle exceeds the critical velocity and ultimately with any further rise in flow speed, the tube's magnitude of vibration grows exceptionally. The major work that is performed on flow-induced vibration (FIV) comprises of the plain tube's vibration exploration encountered with a single and two-phase flow of water, Water and refrigerant. Nowadays, finned tubes are used as a part of heat exchangers in preference to plain tubes and their utilization is probably going to expand more in future.

The failure of heat exchanger tubes is common and it is due to the cause of flow induced vibrations. Such vibrations should be taken at the design stage to ensure good performance and reliability. There are five excitation mechanisms due to which fluid induced vibrations occur. Among such mechanisms causing flow induced vibrations, fluid elastic instability causes the most violent vibrations and may lead to rapid tube failures within short time. The flow induced vibration has been studied since 1970s. The various experimental studies carried out until now, on fluid induced vibration are constantly added new findings into it, which is beneficial for improving design criteria for tube and shell type heat exchangers. In flow-induced vibrations, tube bundles get damaged over a long period of time due to turbulent

buffeting or they can produce high levels of noise due to acoustic resonance. When cross flow velocity in tube bundle exceeds the critical velocity; fluid elastic instability occurs in the tube bundle. The resulting vibration amplitudes of the tubes dramatically increase with increasing flow velocity and rapid tube failures can occur within an hour.

Connors H. J. (1970) did experiments on a cascade of cylinders and using the quasi- static assumption determined the fluid loading due to the static displacement of the cylinder from its original position. Connors defined the phenomenon as “fluid elastic instability” and generated the equation.

Shell and tube heat exchangers are common mechanical equipments utilized in nuclear power, petrochemical, pulp and paper industries, food industry, chemical, and power plants. When the fluid forces cause excessive vibrations of the heat exchanger tubes, tube to-tube clashing may occur and premature tube failure may arise due to fatigue or fretting wear. As such, flow-induced vibration is an important design concern, especially in the nuclear power industry due to the strict safety regulations and the extremely high cost of unplanned plant shutdown and repair.

Flow induced vibrations in structures is caused due to the different five mechanisms namely i) Turbulent Buffering, ii) Vortex Shedding, iii) Jet switching, iv) Acoustic Resonance, v) Fluid elastic instability. Out of different mechanisms of flow induced vibrations, fluid elastic instability mechanism is very crucial mechanism. Fluid elastic instability has been recognized as a major cause of failure in shell and tube type heat exchangers due to tube repwaters and plant down time. Damage caused by first four mechanisms is in over the service of years, but damage caused by fluid elastic instability is in matter of hours. Fluid elastic instability causes sudden and huge failure of heat exchanger. Therefore, fluid elastic vibrations in heat exchanger tube arrays are required to be predicted so that same can be taken into account during mechanical design of the heat exchangers without compromising their thermal performance have described estimation of Fluid elastic instability in tube arrays by using numerical approach. The fluid elastic forces are approximated by the coupling of unsteady flow model with CFD. The effect of pitch to diameter ratio, Reynolds number on FEI threshold was also investigated For plain tube bundles of heat exchanger, much research is conducted over the past 40 years and given design guide-lines to prevent fluid elastic instability in heat exchanger tube arrays. A rare study is carried out for fluid elastic instability in finned tube.

- **Turbulent Buffering:-**

The tubes in tube-and-shell heat exchangers act as turbulence generators and thus, at all practical Reynolds numbers, will be subjected to broad band turbulent buffeting. The nature of this buffeting and its relation to resonant tube vibration and acoustic resonance has been the subject of considerable controversy, the history of which is well covered by Pa'idoussis.

- **Vortex Shedding:-**

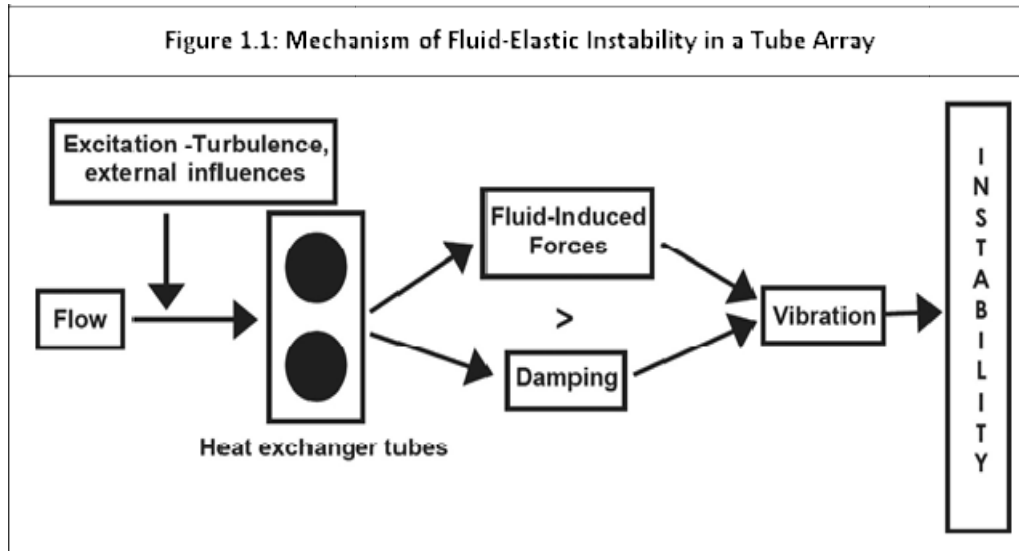
In fluid Dynamic vortex shedding is an oscillating flow that takes place when a fluid such as water flows past a bluff (as opposite to streamlined) body at a certain velocities depending on the size and shape of the body.

- **Acoustic Resonance:-**

Acoustic resonances may occur in heat exchangers with high velocity gas cross flows and are invariably associated with acoustic standing waves at right angles to both the tubes and the mean flow direction. While the problem may manifest itself in the form of excessive noise levels, often exceeding 160dB, it may also lead to substantial structural damage to tubes or ductwork. Pa'idoussis' review outlines many of the uncertainties and controversies which existed at that time. Some interesting progress has been made in the intervening years.

### **Fluid Elastic Instability:**

The phenomenon of fluid elastic instability can be described as a mechanism between tube motion and fluid forces. When a tube bundle is subjected to cross flow, the tubes vibrate with an amplitude proportional to the upstream flow velocity until the flow velocity reaches a threshold limit called the critical velocity where the tube's response amplitude increases dramatically, potentially causing catastrophic failure. From a mechanistic view, the flow field around an array of flexible tubes causes the tube to be displaced from its initial position. This displacement causes a further shift in flow field changing the fluid forces acting on the tubes. The damping force of the tube that tries to restore it back to its equilibrium position opposes this change in fluid force.



Thus, a competition results between the energy input by the fluid force and the energy expended in damping. When the energy expended in damping is more than the energy input by the fluid, the vibrations die down. However, if the fluid forces dominate, sufficient energy is imparted to the tube to sustain the vibrations and an unstable situation is reached where the tube vibrates with large amplitude. In tube heat exchangers, this limit is known as fluid- elastic instability and leads to tube damage. A schematic of this mechanism is shown in Figure1.1.

## 1.2 Relevance:

- Aim of our project is to identify critical velocity at instability due to fluid elastic instability. (Connors, 1978) did experiments on a cascade of cylinders and using the quasi-static assumption determined the fluid loading due to the static displacement of the cylinder from its original position. Connors defined the phenomenon as “fluidelastic instability” and generated the equation.

$$\frac{V_c}{F n . D} = K \times \left[ \frac{m . \delta}{\rho . D^2} \right]^\alpha$$

Where, K is threshold instability constant also known as Connors constant depends on tube pattern and tube spacing. In the above equation,  $V_c/(F n . D)$  the reduced velocity factor and  $K \times \left[ \frac{m . \delta}{\rho . D^2} \right]^\alpha$  is a mass damping parameter. From the above equation, critical velocity ‘ $V_c$ ’ is directly proportional to the natural frequency of tube ‘ $F n$ ’, the mass of tube ‘ $m$ ’ and logarithmic decrement of

finned tube “ $\delta$ ”. The effective diameter “ $D$ ” is the mean diameter of the tube considering the effect of the fin. This equation is used as base for design of experiment and study of instability at velocity. For the experimentation, water is considered for cross flow on tube array.

- Use of fins on the surface of tube is increased in recent days and it is to increase more in future. Due to ability to increase thermal performance, it is necessary to know the effect of water cross flow over tubes having fins on their surface, on the vibration induced by fluidflow.
- Flow-induced vibration is an important design concern, especially in the nuclearpower industry due to the strict safety regulations and the extremely high cost of unplanned plant shutdown and repair.

### 1.3 Objectives :

The aim behind this work is to analyze fluid elastic vibration experimentally with rotated triangular finned tube array subjected to water cross flow. (Sandeep R. Desai & Kengar, 2019; Sandeep R. Desai & Maniyar, 2019; Sandeep R. Desai & Pavitran, 2017) have carried out work on plain and finned tubes with different pitch ratios with parallel triangular, normal triangular tube arrays and rotated triangular tube array for water cross flow. After review of this work, it is decided to carry out the dissertation work for the effect of lower tube array pitch ratio, change in fin density and change in fin height on the instability threshold. The obtained results from this work are converted to dimensionless form.

- To provide guidelines for design of fin tube type shell and tube heat exchanger for failure of tube array.
- To study different flow induced vibration mechanism responsible for failure of tube array.
- To investigate fluid elastic instability in ‘Square finned tube array’ for pitch ratio less than two.
- To investigate the effect of fin pitch density and fin height on critical velocity.

#### **1.4 Methodology and Action plan:**

- Problem identification.
- Preparation of draft for paper publication.
- Review of literature and selection of proper methodology.
- Design and development experimental facility.
- Identify and analyze effect of finned tube and plane tube on Fluid Elastic Instability.
- Experimental investigation of fluid instability in fin tube array for air crosses flow.
- Find out best suitable condition.
- Presentation and submission of report.

## **2. LITERATURE REVIEW.**

### **2.1 Present Theories and practices:**

#### **Sandeep rangrao desai sampat pavitran (2016) ( 1 ) :**

Investigated an experimental program is carried out to determine the critical velocity at instability for plain and finned tube arrays subjected to cross flow of water. The objective of research is to determine the effect of increase in pitch ratio on instability threshold for plain tube arrays and to access the effect of addition of fins as well as increase the fin density on instability threshold for finned tube arrays. The instability threshold for finned tube arrays with fin pitch is delayed compared to coarse fin pitch and hence for increased fin density, the instability threshold is delayed. The experimental results in terms of critical velocities obtained for different tube arrays subjected to water cross flow will serve as the base flow rates for air water cross flow experiments to be conducted in the next phase.

#### **Sandeep r. desai s. pavitran (2013) ( 2 ) :**

Reported failure of tubes in shell and tube heat exchanger is contributed to the cause of fluid induced vibrations leading to production loss and leakage of hazardous fluid flowing inside the tubes out of various mechanism of fluid induced vibrations fluid elastic instability is the most dominant one and causes vibrations of damping nature due to cross flow of fluid over the tubes which is much more considerable than axial flow inside the tubes. Prediction of such vibrations through their analysis requires experiments on fluid elastic vibrations to be conducted to determine critical velocity of fluid at instability threshold. One of the key issues in experiments on fluid elastic vibrations is to model the fluid and structure to simulate fluid elastic vibrations in a heat exchanger tube arrays. This involves design of an experimental setup by considering both structural modeling and fluid modeling requirements.

#### **Jiang lai lei sun lixia gao pengzhpu li( 3 ) :**

Worked to facilitate obtaining the fluid elastic instability mechanism of the tube bundles, a tube system considering cross flow effects is adopted in this paper. The intrinsic mechanism of the fluid force effects on the motion stability of the tube array, at the low flow velocity was relieved. Also, the formula for calculating the critical flow velocity was derived. The results indicate that when the system damping of a tube array is small, the flow velocity reaches a certain value, the fluid elastic

stability of the tube array reaches a critical state, and the first dynamic bifurcation occurs. The fluid elastic instability occurs again as the flow velocity keeps increasing, which was called as the second dynamic bifurcation. When the system damping of a tube array is big, there would be only one dynamic bifurcation, and the tube system reaches the first critical state. The analysis has demonstrated that the higher one is controlled by stiffness mechanism.

**Sandeep r Desai s pavitrn 2017 ( 4 ) :**

Analyzed the present experiment used plain and finned tubes arrays exposed to water cross flow. The parallel triangular array with cantilever end condition is considered for the study. Pitch ratios considered are 2.1 and 2.6 while fin densities considered are 4fpi and 10 fpi l. The parameters measured are water flow rate, natural frequency, and vibration amplitude of the tubes. The datum case results were first obtained by testing plain arrays with pitch ratios 2.1 and 2.6. this was then followed by experiments with finned arrays with pitch ratios 2.1 and 2.6., and each of the tube densities. The results concluded that finned arrays are more Stable in water cross flow compared to plain arrays. The strouhal numbers corresponding to small peaks observed before fluid elastic instability are computed and compared with expected ones according to Owen's hypothesis. It was attributed that peaks observed are attributed to vortex shedding observed for all the arrays tested in water. It also concludes that the critical velocity at instability threshold increases for tubes with fins compared to plain tubes and it further increases with increase in fin density. In this Connor's constant  $K=3$  is taken and results are plotted to determine the values falls in stable region or unstable region.

**Sandeep r desai Rohit kengar (2019)( 5 ) :**

Investigated the research was aimed at determining failure of shell and tube heat exchanger tubes due to flow induced vibrations caused by shell side cross flow. Fluid elastic instability, vortex shedding, and turbulent buffeting are the excitation mechanism responsible for failure of the tubes. The present research work deals with the determination of critical velocity at instability for rotated square finned tube arrays subjected to water cross flow. In all, total six tube arrays are tested with two each with plain, course, fine finned tube arrays. Pitch ratio considered are 2.1 and 2.6 while densities considered are course (4fpi) and fine(10fpi). The effect of array pattern, pitch ratio, and gin densities on the onset of instability is studied by conducting experiments in the water cross flow. The effect of tube array pattern is studied by comparing results of present study with authors published results for parallel triangular finned tube arrays in water cross flow. From the results concluded that addition of



fin on the surface of plain tubes resulted in delay in instability threshold was further delayed due to increasing fin density from course to fine. The fluid elastic instability of finned tube arrays in water was observed to be array geometry dependent. The effect of higher tube array pitch ratio is found to reach instability at comparatively higher pitch velocities for plain, course, as well as fine finned tube arrays.

**Sandeep r desai aslam a maniya(2019-1) ( 6 ) :**

In this experimental program was carried out by subjecting normal square finned tube arrays to gradually increasing water cross flows. In all, total six tube arrays were tested; three having pitch ratios 2.1 and remaining three of pitch ratios 2.6. under each category three arrays tested were plain array coarse finned array and fine finned array. Experiments conducted to study vortex shedding and fluid elastic vibration behavior of plain and finned tube arrays in water. A comparison between vibration response of plain and finned tube arrays indicate that fluid elastic instability occurs early for plain tube arrays. The strouhal numbers computed for different tube arrays shows that the values are less for finned arrays compared to plain arrays. From Connor's constant values of both normal square arrays and parallel triangular arrays pattern Connor's constant values for normal square pattern are more stable than parallel triangular arrays pattern.

**Pravin h yadav dilip Kumar Mohanty( 7 ) :**

In this experiment the program was conducted to obtain fluid elastic instability in a parallel triangular tube array subjected to water cross flow, an experimental procedure was carried out. Effect of tube material for bare tube and fin tube with 3mm fin height 8.47 mm pitch is analyzed with pitch ratio 1.79. Tubes of steel, aluminum and copper Material are considered for study. Fluid elastic instability is compared with tubes of different materials. This shows that fluid elastic instability is dependent on tube material density. For tube material with higher density, fluid elastic instability is delayed compared to tubes with low density are more stable against fluid elastic instability. From Connor's instability map it is observed that aluminum tube arrays are more unstable as compared to steel and copper tube arrays. For each tube array pattern, before occurrence of instability a small pick was observed which further needed to check by strouhal equation.

**G. Ricciardi, M.J. pettigrew, N.W..Mureithi( 8 ) :**

Investigated that two phase flow in steam generators can induce tube vibrations that may cause fretting-wear and even fatigue cracks. It is important to understand the relevant two phase flow induced vibration mechanism. The results of the vibration of a normal triangular tube bundles subjected to air-water cross flow. The pitch to diameter ratio is 1.5 and tube diameter is 38mm. Tubes

were flexible in one direction, the lift and drag direction were tested. Fluid elastic instabilities and tube resonances were observed. The resonances induced significant vibration amplitude at high void fractions in the lift direction. The results are compared with those obtained with the rotated triangular tube bundle, and showed that the normal triangular configuration is more stable than the rotated triangular configuration.

**Vikram B Yadav, S.R. Desai, M. M. Mirza( 9 ) :**

Investigated that major failure of shell and tube type heat exchangers in short time is caused due to fluid elastic instability. Due to fluid elastic instability vibrations, short term failure of heat exchanger tube bundles occurs by fatigue and wear. Here experiments carried out for critical reduced velocity for in line square tube array and rotated square tube arrays of finned tubes. While addition of fins to in line square tube array the critical velocity is delayed becomes less well defined. The addition of fins to the rotated square tube array, appears to reduce the fluid elastic threshold value and make it more clearly defined

**H. Arshad, S. Khushnood, L. Ahmad Nizam, M. Amir Ahsan, O. Ghufraan Bhatti( 10 ) :**

Investigated an experimental study is carried out on a parallel triangular finned tube array with P/D ratio 1.62 to examine the effect of fin geometry on flow induced vibrations response. Fins on the tubes increase the heat transfer rate but these also affect the fluid dynamics around the tubes. There are numerous parameters that affect the finned tube vibration subjected to air cross flow in tube array. The current experimentation is performed in a subsonic wind tunnel using a single flexible aluminum finned tube in a rigid array. It has been observed that during spectral analysis that the Strouhal number is independent of fin geometry since it remained constant in different rows of the array for finned tube under study. It suggests that the vortex shedding has also contributed towards the finned tube vibrations predominantly in the first, second and the fourth row of tube array.

### 3. DESIGN AND MODIFICATION OF TEST SETUP.

#### 3.1 Experimental Facility Available:-

The line sketch of facility is given in figure 1. The main parts of the tunnel are numbered and named below the figure. The nominal dimensions of the facility are marked on the figure. The specifications of the facility are also given below.

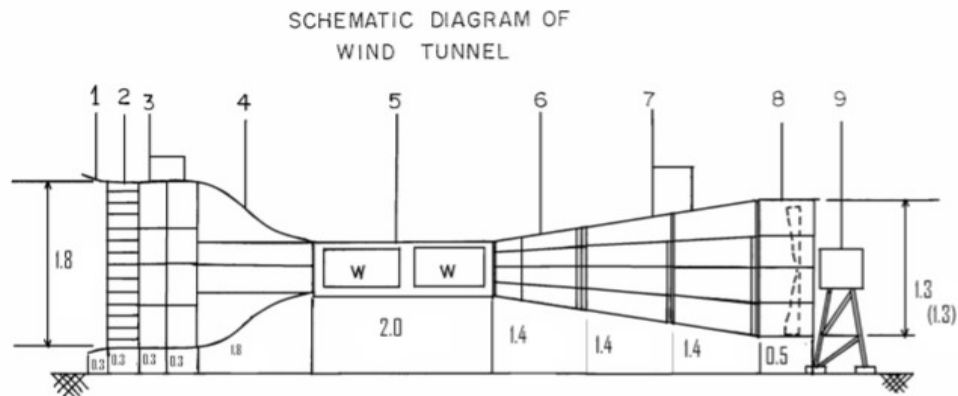


Fig 3.1: Schematics of the wind turbine.

Table 3.1: Specification of Wind Turbine

Sr.No.	Title	Specification
1.	Test Section Size	Cross Section: 600mm×600mm Length: 2000mm.
2.	Maximum Speed	50m/sec.
3.	Fan	Axial Flow fan of Diameter: 1.3 meter. Maximum rpm: 1400 Number of Blades: 12

4.	Contraction Ratio	9: 1
5.	Contraction length	1.8m
6.	Settling chamber	1800mm×1800mm
7.	Entry section	Bell mouthed entry
8.	Honey Comb Size	25mm×25mm×200mm
9.	Screens	Two screens 8mesh and 16mesh stainless steel
10.	Provision to put smoke rake	provided in the contraction cone
11.	Power	22KW AC motor, with speed control drive

### 3.2 Experimental Setup:

The test section has four Perspex windows for viewing inside the test section. The top can be easily access to the test section so that it becomes convenient to set up experiments.

The fabrication of the tunnel is made using teak wood and airproof plywood. The diffuser has a transition piece with square inlet and circular outlet. The diffuser angle is less than 9°so that separation is avoided in the diffuser. The speed of the tunnel can be varied continuously from 3 to 50m/sec. However continuous running of the tunnel is possible from 3m/sec to 50 m/sec. Below 3 m/sec speed the tunnel should not be run continuously, but can be run for very short durations only (the motor will get heated up if run for long duration at low RPM). These short duration runs can be intermittent allowing enough time for motor to cool in between.

A single channel electronic manometer is used to measure pressure and velocity. Pitot tube is placed in front of tubes whose other end is single channel electronic manometer. single channel electronic manometer has two inputs one from pitot tube and other is from atmosphere with the help of

tube, placed open to atmosphere. single channel electronic manometer gives direct output in terms of velocity and pressure.

The tunnel is operated from range 100 rpm to 1300 rpm. The speed of tunnel is obtained by varying rpm of fan. The fan is directly coupled to an AC motor whose speed can be varied using an AC motor controller.

The test section of tunnel is 600\*600\*2000mm we gave made another test section inside the wind tunnel test section. The fabrication is made from the plywood. This modification was done because the original test section is too large and for that section it requires more tubes for testing For our testing we have 9 tubes of one set. So it requires smaller section of dimension 600\*600\*300mm.

The accelerometer 7401 is connected to the tube in 3<sup>rd</sup> row 2<sup>nd</sup> position and other end connected to the data acquisition system DEWE SOFT 7.1.1 which directly gives readings in the form of graph.

#### **Modification in experimental setup:**

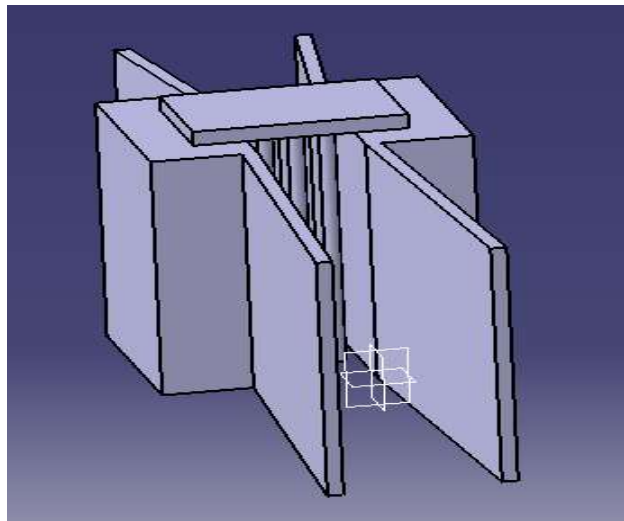


Fig 3.2: Modification in Wind Turbine

The test section of tunnel is 600\*600\*2000mm we gave made another test section inside the wind tunnel test section. The fabrication is made from the plywood. This modification was done because the original test section is too large and for that section it requires more tubes for testing For our testing we have 9 tubes of one set. So it requires smaller section of dimension 600\*600\*300mm.

### Selection of the Tube Array Pattern:

In the following Fig .1, normal tube arrays are shown. From this, it is clear that in normal square tube array, holes made on the pattern are at  $90^\circ$  to each other. And in this case of normal square tube array they are at  $90^\circ$ . So, these are the made in the present tube array pattern on front and back plates while maintaining the required pitch ratio. Determined instability threshold forth is tube array pattern will be compared with earlier published results of tube array patterns. It will help us to know which of the tube arrays is having more stability to fluid induced vibrations.

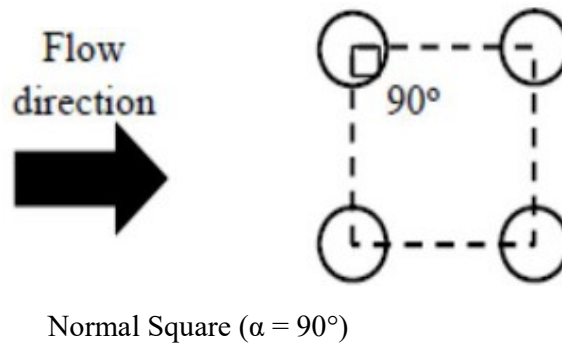


Fig 3.3: Tube Array Configurations

### Number of Tubes :

For present study, pitch ratio considered is 1.78 for air cross flow. Because, after calculation of critical velocities at instability for other pitch ratio greater than this, there was a problem with flow capacity of the pump required to lift the air with available experimental setup. Hence are likely top problems for experimental simulation of fluid elastic instability. According to previous research when pitch ratios are more than the 2.6, then it effects on the instability threshold frequency. Therefore, according to centrifugal pump capacity it is, decided to go with pitch ratio less than 2.6.

There are nine tubes selected for the experimentation, because more number of tubes and larger tube array will increase the test section area leading to lower gap velocity for the same volumetric flow rate of air or air-air. This will pose problems in experimentally achieving instability thresholds for tube array under consideration. To experimentally achieve instability threshold point ,the natural frequency and logarithmic detrimental so should below. This is kept in mind while selecting tube length, rod length and tube diameter and tube material. The natural frequency depends on all these parameters.

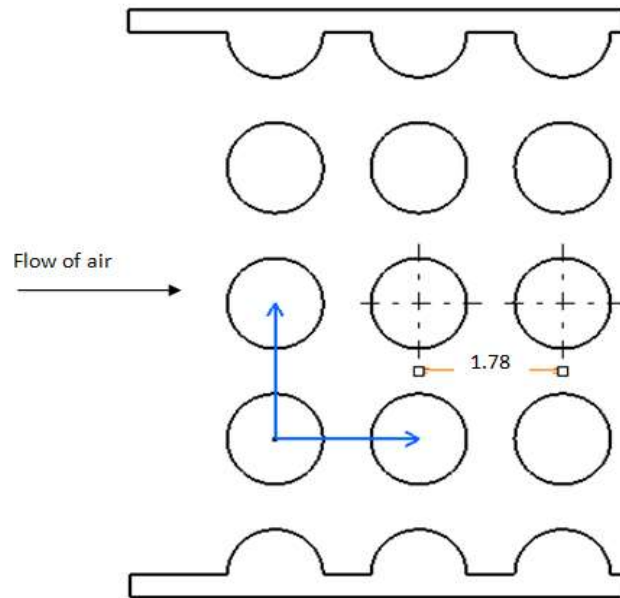


Fig 3.4: Arrangement of tubes during the experimentation across the flow.

## 4 FREE VIBRATION TESTING.

### 4.1. Data Acquisition System:

Data Acquisition System comprises of acquiring data from the different transducer and signal conditioner and enables the user to do processing, storage, and analysis. The main purpose of DEW Soft is to have two modes of operation: Acquisition and Analysis. The main difference is that the Acquisition part works with real hardware while Analysis works with the stored file. But the same math processing and visualization can be applied either during measurement or also on stored files. It is used for seeking the results of the natural frequency of any structure with the help of a free vibration analysis setup. With the help of this analysis, the damping of the structure is also calculated. The 8-channel data acquisition consists of a hardware element (Dewtron Data logger, accelerometer) and the software element is (Dew soft 7.1.1). The measurement system and its specifications are shown in Table 4.1 and Table 4.2. In Table 4.1 show all details and specification of accelerometer

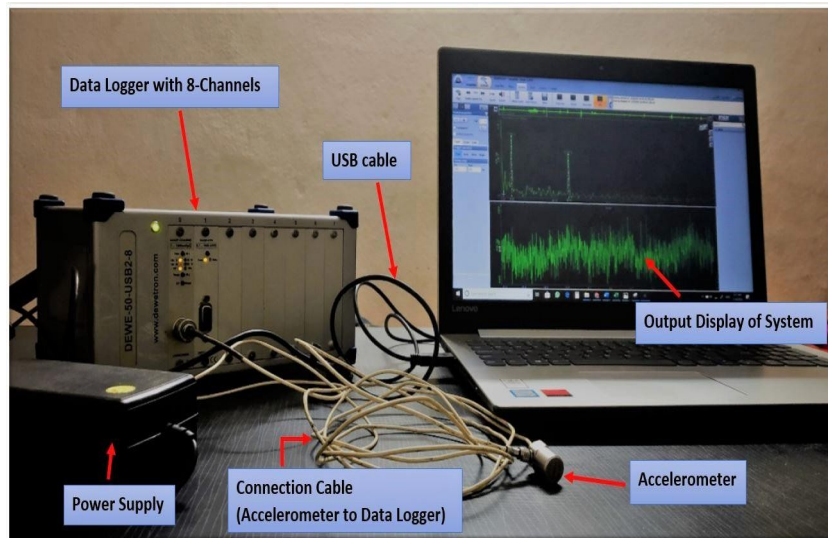


Figure 4.1: Setup of Data Acquisition System.

Table 4.1 and 4.2 includes the details and specification of 8-channel data logger data acquisition system.



Table 4.1: Specification of Accelerometer(DYNAMIX 6503)

Sensitivity, 5%	20 pc/g
Range F. S.	2000g
Frequency response, 5%	0.5 to 10,000 Hz
Resonant frequency	40,000 Hz
Maximum transverse sensitivity	5%
Non- linearity	±2
Weight	14 g
Shock max	2,000
Temperature range	0 to 250

Table 4.2: Specification of Data Acquisition System

Number of channels	8
Measured values	According to installed DAQP modules
Resolution	24 bit based on internal A/D system
Type of ADC	Delta-sigma
Sampling rate	204.8kS/s
-3 dB bandwidth	<a href="#">76kHz@204.8kS/s</a>
Accuracy	0.05% of range, mV
Signal to noise @ fs1000Hz	100dB
Crosstalk	100dB
Power supply	9 to 36 V
Counter modes	Event counting, cycle,
Resolution	32 bit based on digital inputs
Tim base	102.4 MHz
Signal levels	30 V

## 4.2 Free Vibration Analysis:

According to Connors' equation for conducting the experiments on fluid elastic vibrations at the lower flow rate, the natural frequencies of the structure should be as minimum as possible. As critical velocity is directly proportional to natural frequency and effective diameter, therefore, to get the critical velocity at instability at a lower flow rate the natural frequency of the setup has to be lowered. The natural frequency of a system depends on the size and shape i.e. geometry, boundary conditions, and material property of the system. For reducing the natural frequency of the finned tube, there is constrained on the boundary condition and the material of the finned tube. For this analysis, the base design is chosen from the work of Desai and Pavitran, and Desai and Maniyar. Desai and Pavitran, Desai, and Maniyar and Desai and Kengar worked on the parallel triangular, normal square, and rotated square tube arrays respectively. The tube array specifications of the experimentation are shown in Table 4.3. Experimental free vibration analyses for the plain and finned tubes are carried out by using a data logger and accelerometer. The natural frequencies of different tubes were found out in the air. The end condition of the tube is cantilever with 1000 mm length. The measurement system of free vibration testing is shown in Fig. 4.2, where finned tubes are tested for damping parameters. The frequency spectrum plots are recorded during the free vibration testing and from these the natural frequency 3mm-9fp is shown in from Fig.4.2.

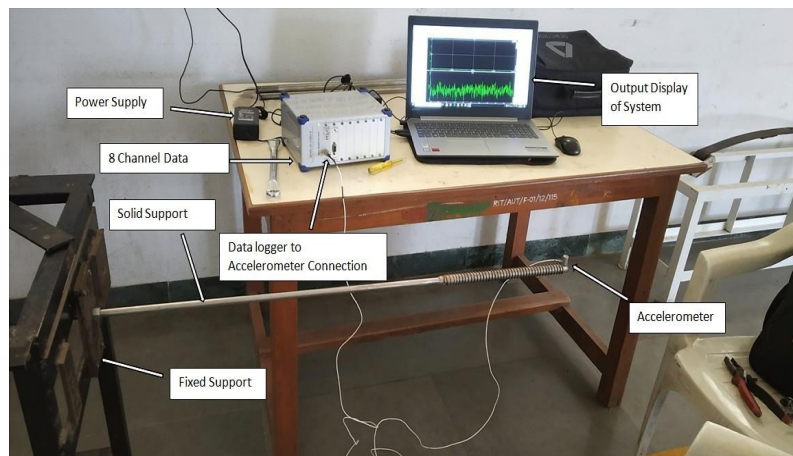


Figure 4.2: Experimental setup for free vibration testing.

Table 4.3: Specification Of Tube Array

Sr. No.	Parameters	Specification	Sr. No.	Parameters	Specification
1	Tube material	Stainless steel	9	Modulus of Elasticity N/m <sup>2</sup>	1.9x10 <sup>11</sup>
2	Density, Kg/m <sup>3</sup>	7850	10	No. of tubes	9
3	End condition	Cantilever	11	Fin height, mm	3 and 6
4	Tube O.D, mm	19.05	12	Fin thickness, mm	0.5
5	Tube I.D, mm	15.05	13	Fin pitch, mm	3 fpi, 9 fpi
6	Fin type	Spiral	14	Finning length, l, mm	590
7	Fin material	Stainless steel	15	Support rod diameter, mm	14.5
8	Type of array	Square	16	Support rod length, mm	10

### 4.3 Determination of Damping Ratio:-

**Finned Tube: Fin Height: 3mm, Fin Pitch: 2.82mm:**

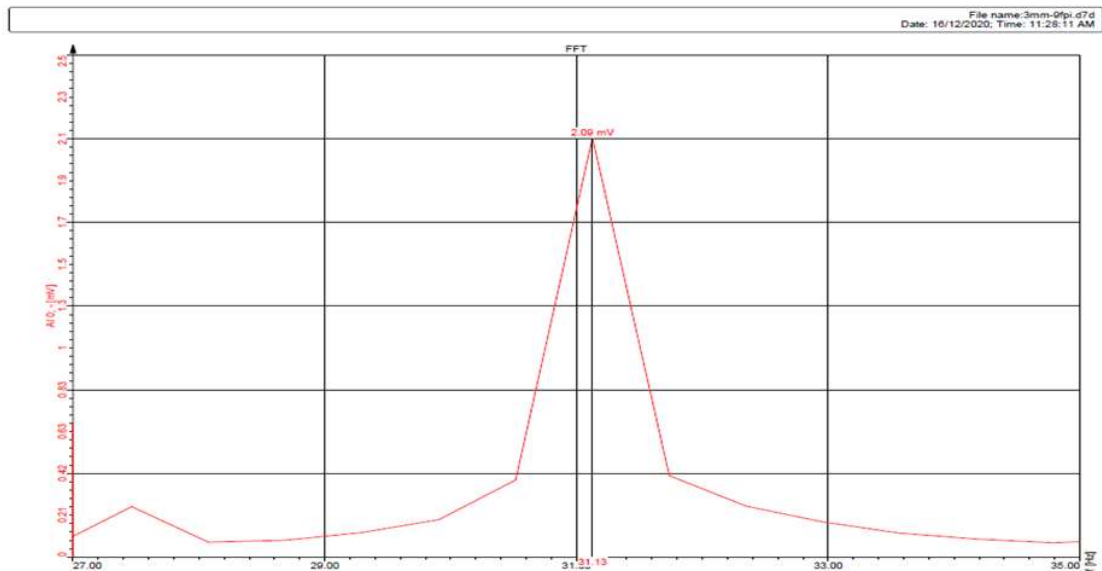


Fig 4.3 : Frequency spectrum of natural frequency for 3mm 9fpi

- Fn- 31.13Amp.- 2.09

Using half band width method we can calculate f1 and f2 values by intersecting line of amplitude at distance of  $\frac{\text{height of amplitude in mm}}{\sqrt{2}}$  and getting values on frequency line

$$\begin{aligned}\zeta &= \frac{1}{2} \left( \frac{f_2 - f_1}{f_n} \right) \\ &= \frac{1}{2} \left( \frac{31.30 - 30.90}{31.13} \right) \\ &= 0.0064 \\ \delta &= \frac{2\pi \times \zeta}{\sqrt{1 - \zeta^2}} \\ &= \frac{2\pi \times 0.0064}{\sqrt{1 - 0.0064^2}} \\ &= 0.0402\end{aligned}$$

Similarly, Natural frequency and Logarithmic decrement for all tubes,

Table 4.4: Results of Natural frequency and logarithmic decrement for free vibration testing

Type of Tube (Fin Height- Fin Density in inch)	Natural Frequency ( $f_n$ )(Hz)	Damping Factor ( $\zeta$ )	Logarithmic Decrement ( $\delta$ )
Plain	35.40	0.0092	0.0576
3 mm 3fpi	34.80	0.0074	0.0469
3 mm 9fpi	31.13	0.0064	0.0402
6 mm 3fpi	32.35	0.0057	0.0358
6 mm 9 fpi	29.30	0.0080	0.0505

## 5. EXPERIMENT IN AIR CROSS FLOW

### 5.1 Experimental procedure:

The plain or finned tube arrays are inserted inside the test section and actual testing with plain or finned tube bundles is carried out as follows :-

1. Insert the set of array inside the test section and place the accelerometer at the third row middle tube.
2. The pitot tubes one end is placed in front of flow of air and other end is connected to single channel electronic manometer.
3. Increase the rpm from 100 rpm to 1300 rpm with the help of AC motor controller.
4. Also for every set of array record the readings from range 1300rpm to 100rpm.
5. Output from accelerometer is recorded with the help of data actuation system which directly gives readings on DEWE SOFT software.
6. The recorded data from DEWE SOFT 7.1.1 is used to process data obtained from accelerometer and signal conditioner.
7. The software gives readings in the form of graph (frequency vs amplitude).
8. The data is processed to identify critical velocity at instability for tube array under – consideration.

### 5.2 Measurement Methodology:

The parameters obtained by free vibration analysis earlier are used to evaluate the fluid elastic instability in normal square tube array pattern. The prerequisite parameters required for results analysis and this analysis is done for 1.78 pitch ratio.

- **Determination of Damping Ratios:**

**Finned Tube: Fin Height: 3mm, Fin Pitch: 2.82mm:**

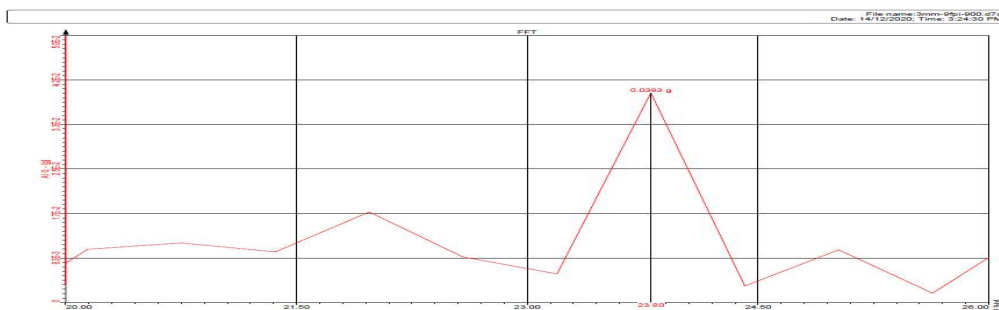


Fig 5.1: Frequency spectrum of Forced vibration for 3mm 9fpi

- Fn- 23.80Amp.- 0.0393

Using half band width method we can calculate f1 and f2 values by intersecting line of amplitude at distance of  $\frac{\text{height of amplitude in mm}}{\sqrt{2}}$  and getting values on frequency line

$$\begin{aligned}\zeta &= \frac{1}{2} \left( \frac{f_2 - f_1}{f_n} \right) \\ &= \frac{1}{2} \left( \frac{31.30 - 30.90}{31.13} \right) \\ &= 0.0064 \\ \delta &= \frac{2\pi \times \zeta}{\sqrt{1 - \zeta^2}} \\ &= \frac{2\pi \times 0.0064}{\sqrt{1 - 0.0064^2}} \\ &= 0.0402\end{aligned}$$

Similarly, Natural frequency and logarithmic decrement for all tubes,

Table 5.1: Result of Natural frequency and logarithmic decrement for Forced Vibration

Type of Tube (Fin Height- Fin Density)	Natural Frequency ( $f_n$ )(Hz)	Damping Factor ( $\zeta$ )	Logarithmic Decrement ( $\delta$ )
Plain	25.02	0.0064	0.0402
3mm 3fpi	21.97	0.0129	0.0814
3mm 9fpi	23.80	0.0084	0.0527
6mm 3fpi	25.02	0.0086	0.0540
6mm 9fpi	25.63	0.0095	0.0597

- **Effective diameter:-**

The effective diameter is calculated by equation

$$D_{eff} = \left[ \frac{t}{p} (D_f - D) + D \right]$$

Where p is the fin pitch, t is the fin thickness, D-f is the fin diameter, and D is the bare tube diameter

- **Total mass- ( M ) :**

Total mass of tubes is equal to structural mass.

$$\text{Structural mass} = m_s = \rho \cdot v = \rho \left( \frac{\pi}{4} D_{eff}^2 - \frac{\pi}{4} d_i^2 \right)$$

Total Mass,

$$M = M_s$$

Effective diameter and Total mass for all tubes,

Table 5.2: Result of Effective Diameter and Total mass

Tube Geometry (Fin Height- Fin Density)	Total Geometry (Kg/m)	Effective Diameter (m)
Plain	0.8410	0.01905
3 mm 3 fpi	0.9239	0.01940
3 mm 9 fpi	1.0969	0.02011
6 mm 3fpi	1.0084	0.01975
6 mm 9 fpi	1.3876	0.02125

- **Amplitude in mm :**

Height of amplitude in mm of Frequency for all tubes can calculated using formula,

$$\text{Amplitude in } mm = \frac{\text{Amplitude} \times g}{(2\pi \times f_n)^2} \times 1000$$

- **Amplitude Ratio:**

Amplitude ratio is ratio of amplitude in mm to effective diameter of tube,

$$\text{Amplitude ratio} = \frac{\text{Amplitude in } mm}{D_{eff}} \times 100$$

Amplitude in mm and Amplitude ratio for all tubes,

Table 5.3: Results of Amplitude in mm and Amplitude ratio

Type of Tube (Fin Height- Fin Density)	Amplitude in mm	Amplitude ratio
Plain	0.0121	0.0637
3 mm 3 fpi	0.0199	0.1028
3 mm 9 fpi	0.0172	0.0855
6 mm 3 fpi	0.0107	0.0543
6 mm 9 fpi	0.0069	0.0324

- **Reduced Velocity:**

Reduced velocity is evaluated from following equation,

$$v_R = \frac{(v_g)_c}{f_n \times D_{eff}}$$

Where,  $V_R$  is reduced velocity,  $V_g$  is gap velocity,  $F_n$  is natural frequency and  $D_{eff}$  is effective diameter of tubes.

For 3 mm fin height and fin pitch  $p = 2.822$  mm.

$$\begin{aligned} v_R &= \frac{(v_g)_c}{f_n \times D_{eff}} \\ &= \frac{38.77}{23.80 \times 0.02011} \\ &= 81 \text{ m/s} \end{aligned}$$

- **Mass Damping Parameter:**

For 3 mm fin height and fin pitch  $p = 2.822$  mm.

$$\begin{aligned} \text{Mass damping parameter} &= \left( \frac{m \times \delta}{\rho \times D_{eff}^2} \right) \\ &= \left( \frac{1.0969 \times 0.0527}{1.204 \times 0.02011^2} \right) \\ &= 118.72 \end{aligned}$$

- **Threshold Instability Constant:**

Connors defined this phenomenon as “fluid elastic instability” and generated the equation known as Connors equation.

$$\begin{aligned} \text{Threshold Instability constant} = K &= \frac{v_R}{(\text{mass damping parameter})^{\frac{1}{2}}} \\ &= \frac{81}{10.89} \\ K &= 7.43 \end{aligned}$$



## 6. RESULT AND DISCUSSION

To obtain fluid elastic instability in a normal square tube array subjected to air cross flow an experimental procedure was carried out. The results of the experimentation for Plain, 3mm 3 fpi, 3mm 9 fpi, 6mm 3 fpi, 6 mm 9 fpi are shown in table 5.1, 5.2, 5.3, 5.4, 5.5 respectively.

- Results of Plain tube Array:**

Table 6.1: Results of Plain tube Array

Natural frequency (Hz)	Amplitude(g)	Amplitude (mm)	Frequency (Rad/Sec)	Free Stream Velocity(m/sec)	Gap Velocity(m/sec)	Reduced velocity	Amplitude Ratio %
25.02	0.01	0.0040	157.2257	1.8800	4.2756	8.9704	0.0209
25.02	0.0101	0.0040	157.2257	3.7800	8.5967	18.0363	0.0211
25.02	0.0101	0.0040	157.2257	5.7900	13.1679	27.6270	0.0211
25.02	0.0112	0.0045	157.2257	7.7700	17.6709	37.0746	0.0234
25.02	0.0126	0.0050	157.2257	9.8500	22.4013	46.9993	0.0263
25.02	0.0146	0.0058	157.2257	11.9300	27.1318	56.9241	0.0305
25.02	0.0354	0.0141	157.2257	13.9800	31.7940	66.7056	0.0738
25.02	0.118	0.0469	157.2257	16.5000	37.5251	78.7298	0.2461
25.02	0.118	0.0469	157.2257	17.9500	40.8227	85.6485	0.2461
25.02	0.147	0.0584	157.2257	19.9400	45.3485	95.1438	0.3066
25.02	0.213	0.0846	157.2257	22.3900	50.9204	106.8340	0.4443
25.02	0.249	0.0989	157.2257	24.5300	55.7873	117.0450	0.5194
25.02	0.281	0.1117	157.2257	26.4700	60.1993	126.3018	0.5861

- Results of 3mm 3fpi Tube Array:**

Table 6.2: Results of 3mm 3fpi Tube Array

Natural frequency (Hz)	Amplitude(g)	Amplitude (mm)	Frequency (Rad/Sec)	Free Stream Velocity(m/sec)	Gap Velocity(m/sec)	Reduced velocity	Amplitude Ratio %
20.14	0.0165	0.0101	126.5598	1.8800	4.3781	11.2053	0.0522
20.75	0.0176	0.0102	130.3930	3.7800	8.8027	21.8674	0.0524
20.75	0.0189	0.0109	130.3930	5.7900	13.4836	33.4954	0.0563
20.75	0.0207	0.0120	130.3930	7.7700	18.0945	44.9497	0.0616
21.97	0.0258	0.0133	138.0595	9.8500	22.9384	53.8184	0.0685
21.97	0.0293	0.0151	138.0595	11.9300	27.7822	65.1831	0.0778
21.97	0.0403	0.0208	138.0595	13.9800	32.5562	76.3838	0.1071
21.97	0.0387	0.0199	138.0595	16.5000	38.4247	90.1526	0.1028
21.97	0.0467	0.0241	138.0595	17.9500	41.8014	98.0751	0.1241
21.97	0.0564	0.0291	138.0595	19.9400	46.4356	108.9480	0.1498
21.97	0.0673	0.0347	138.0595	22.3900	52.1411	122.3343	0.1788
21.97	0.0825	0.0425	138.0595	24.5300	57.1247	134.0269	0.2192
21.36	0.0882	0.0481	134.2262	26.4700	61.6425	148.7569	0.2479

• **Results of 3mm 9 fpi Tube Array:**

Table 6.3: Results of 3mm 9 fpi Tube Array

Natural frequency (Hz)	Amplitude(g)	Amplitude (mm)	Frequency (Rad/Sec)	Free Stream Velocity(m/sec)	Gap Velocity(m/sec)	Reduced velocity	Amplitude Ratio %
21.97	0.0223	0.0115	138.0595	1.6100	3.9410	8.9199	0.0571
21.36	0.0231	0.0126	134.2262	3.3500	8.2001	19.0901	0.0626
20.75	0.0213	0.0123	130.3930	5.1000	12.4838	29.9169	0.0612
21.36	0.0243	0.0132	134.2262	6.8300	16.7185	38.9210	0.0659
21.36	0.025	0.0136	134.2262	8.6700	21.2225	49.4063	0.0678
21.97	0.0281	0.0145	138.0595	10.4500	25.5796	57.8963	0.0720
23.8	0.0351	0.0154	149.5592	12.2800	30.0590	62.8038	0.0766
23.8	0.0422	0.0185	149.5592	14.0100	34.2937	71.6516	0.0922
23.8	0.0393	0.0173	149.5592	15.8400	38.7732	81.0108	0.0858
23.8	0.0612	0.0269	149.5592	17.5700	43.0079	89.8585	0.1336
23.8	0.0726	0.0319	149.5592	19.3500	47.3650	98.9620	0.1585
23.8	0.0794	0.0349	149.5592	21.0800	51.5997	107.8098	0.1734
23.8	0.096	0.0422	149.5592	23.9700	58.6739	122.5902	0.2096

• **Results of 6 mm 3 fpi Tube Arrays:**

Table 6.4: Results of 6 mm 3 fpi Tube Arrays

Natural frequency (Hz)	Amplitude(g)	Amplitude (mm)	Frequency (Rad/Sec)	Free Stream Velocity(m/sec)	Gap Velocity(m/sec)	Reduced velocity	Amplitude Ratio %
25.02	0.0139	0.0055	157.2257	1.8800	4.2756	8.9704	0.0290
25.02	0.0149	0.0059	157.2257	3.7800	8.5967	18.0363	0.0311
25.02	0.0146	0.0058	157.2257	5.7900	13.1679	27.6270	0.0305
25.02	0.0151	0.0060	157.2257	7.7700	17.6709	37.0746	0.0315
25.02	0.0159	0.0063	157.2257	9.8500	22.4013	46.9993	0.0332
25.02	0.0209	0.0083	157.2257	11.9300	27.1318	56.9241	0.0436
25.02	0.0361	0.0143	157.2257	13.9800	31.7940	66.7056	0.0753
25.02	0.027	0.0107	157.2257	16.5000	37.5251	78.7298	0.0563
25.02	0.0433	0.0172	157.2257	17.9500	40.8227	85.6485	0.0903
25.02	0.0559	0.0222	157.2257	19.9400	45.3485	95.1438	0.1166
25.02	0.0675	0.0268	157.2257	22.3900	50.9204	106.8340	0.1408
25.02	0.0767	0.0305	157.2257	24.5300	55.7873	117.0450	0.1600
25.02	0.0891	0.0354	157.2257	26.4700	60.1993	126.3018	0.1858

• **Results of 6 mm 9 fpi Tube Array:**

Table 6.5: Results of 6 mm 9 fpi Tube Array

Natural frequency (Hz)	Amplitude(g)	Amplitude (mm)	Frequency (Rad/Sec)	Free Stream Velocity(m/sec)	Gap Velocity(m/sec)	Reduced velocity	Amplitude Ratio %
25.02	0.0153	0.0061	157.2257	1.8800	5.0133	9.4293	0.0286
20.75	0.0179	0.0103	130.3930	3.7800	10.0800	22.8604	0.0487
20.75	0.0189	0.0109	130.3930	5.7900	15.4400	35.0163	0.0514
24.41	0.0199	0.0083	153.3924	7.7700	20.7200	39.9451	0.0391
27.41	0.0224	0.0074	172.2444	9.8500	26.2667	45.0959	0.0349
26.25	0.0212	0.0077	164.9550	11.9300	31.8133	57.0323	0.0360
25.63	0.0204	0.0077	161.0589	13.9800	37.2800	68.4492	0.0364
26.25	0.0213	0.0077	164.9550	16.5000	44.0000	78.8796	0.0362
25.63	0.0253	0.0096	161.0589	17.9500	47.8667	87.8872	0.0451
25.63	0.0182	0.0069	161.0589	19.9400	53.1733	97.6307	0.0324
26.86	0.0308	0.0106	168.7882	22.3900	59.7067	104.6063	0.0500
26.86	0.0385	0.0133	168.7882	24.5300	65.4133	114.6044	0.0625
23.8	0.0525	0.0231	149.5592	26.4700	70.5867	139.5683	0.1085

• **Graph of Amplitude vs. Gap velocity for all tube arrays:**

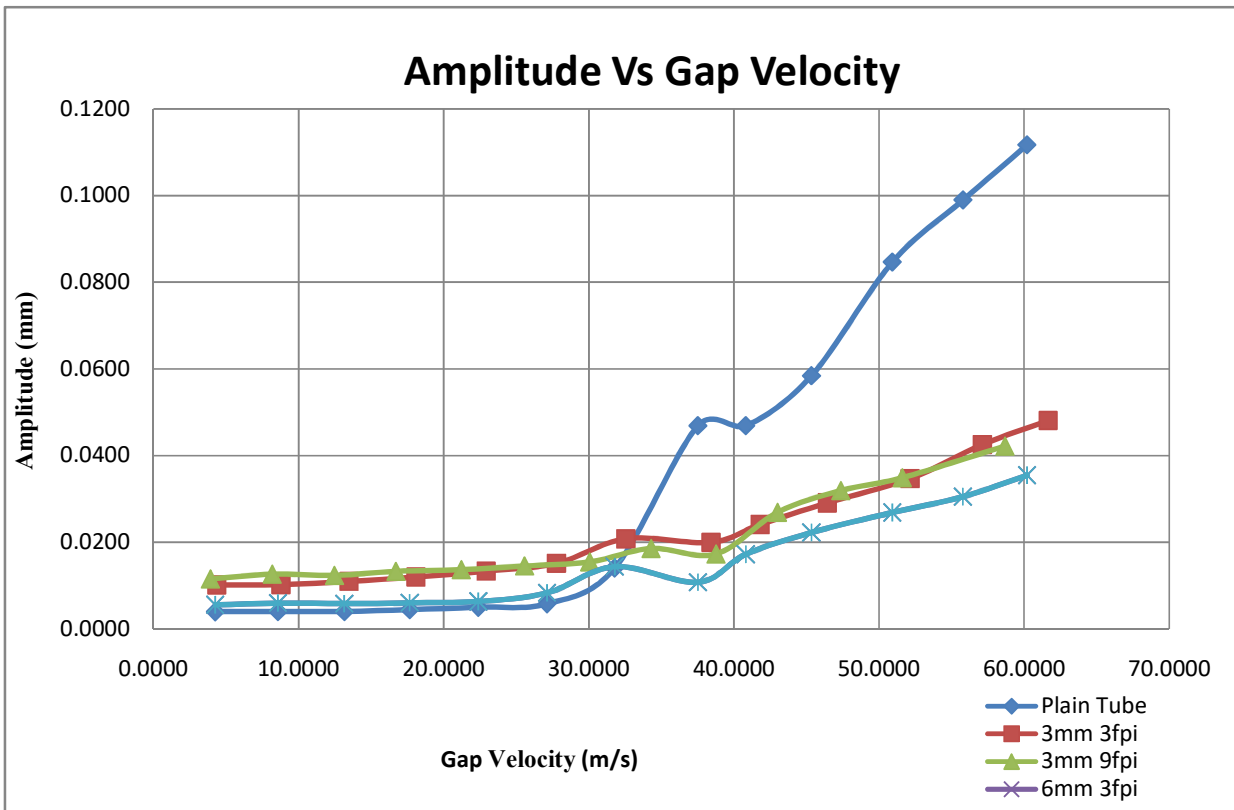


Fig 6.1: Amplitude vs. Gap velocity for all tube Arrays

- **Graph of Amplitude Ratio vs. Reduced velocity for all tube arrays:**

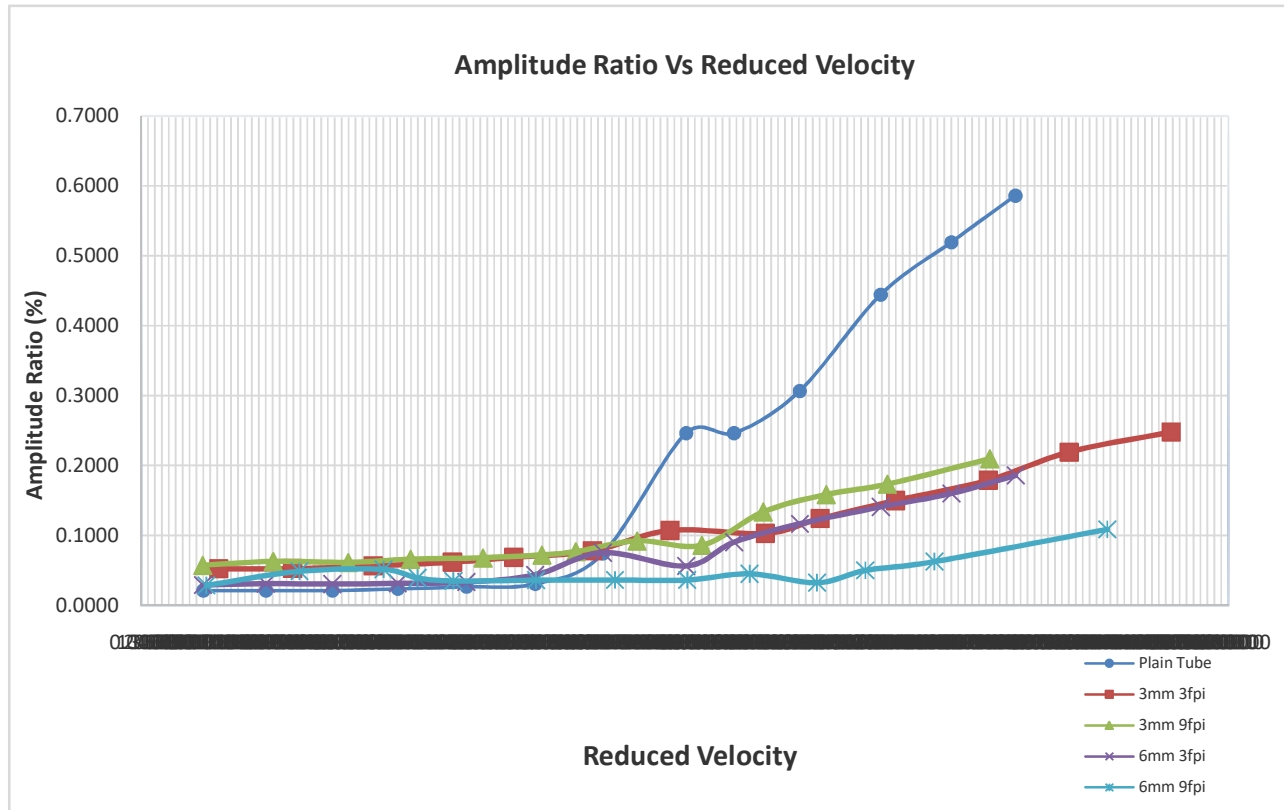


Fig 6.2: Amplitude ratio vs. Reduced velocity for all tube arrays

- **Instability Parameters for all Tube Arrays:**

Table 6.6: Instability Parameters for all Tube Arrays

Type of Tube (Fin Height- Fin Density)	Reduced Velocity	Mass Damping Parameter	K
Plain	85.64	77.26	9.74
3 mm 3 fpi	90.14	165.89	6.99
3 mm 9 fpi	81	91.01	7.43
6 mm 3 fpi	79.66	115.77	7.40
6 mm 9 fpi	97.63	152.27	7.91

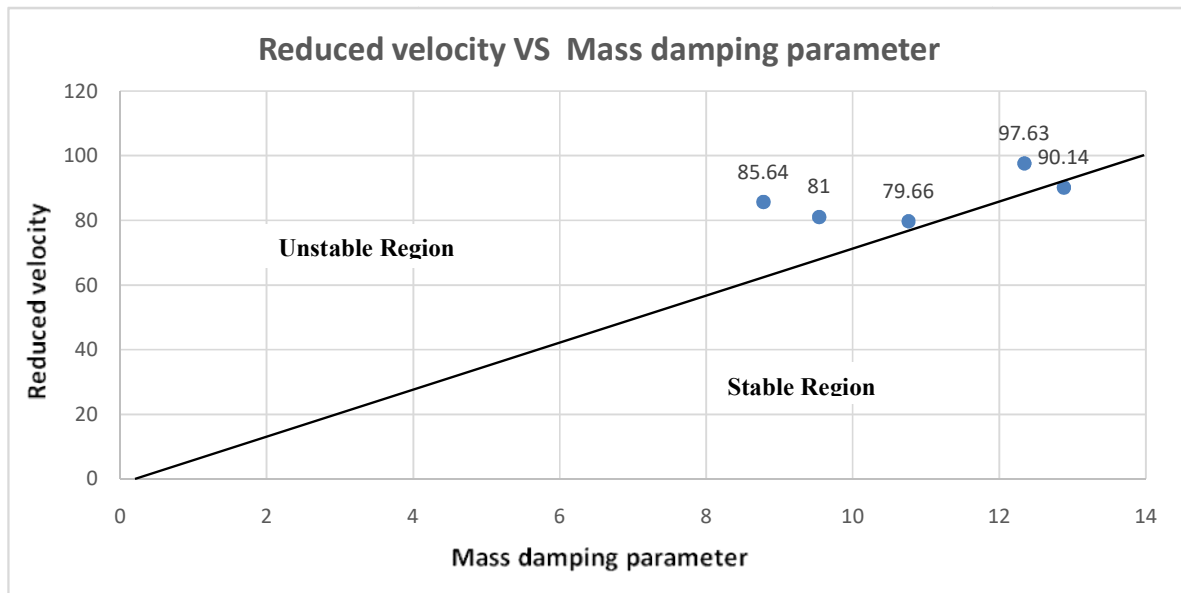


Fig 6.3: Connor's Instability map Mass damping parameter vs. Reduced velocity

## 7. CONCLUSION AND FUTURE SCOPE

### 7.1 Conclusion:

- Critical reduced velocity for finned tubes are increased as increase in fin height and fin density compared to plain tube, but for 3mm 9 fpi and 6mm 3 fpi tube arrays is not obtained due to experimental error.
- .Logarithmic decrement and natural frequency of tube are strongly dependent on tube geometry. With increase in fins on the tube, a decrease in natural frequency observed.
- For each tube array, before the occurrence of instability a small pick was observed which is may be due to vortex shedding which further needed to check by strouhal equation.
- From Connors instability chart it is observed that Plain tube and 3mm 9 fpi tube arrays are more unstable as compared to 3 mm 3 fpi, 6 mm 3 fpi and 6 mm 9 fpi tube arrays.

### 7.2 Future scope:

Scope of project is limited to

1. Experimental testing for study instability of finned tube array with different fin geometry.
2. Compare the results of instability with existing literature.

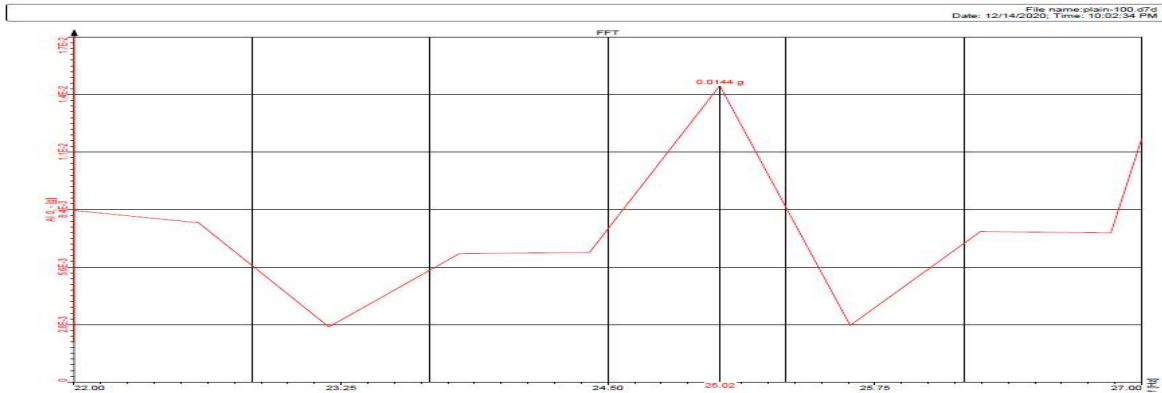
## 8. REFERENCES

1. SandeepRangraoDesai<sup>1</sup> ,Sampat Pavitran<sup>2</sup> (2016) : “The Effect of Fin Pitch on Fluid Elastic Instability of Tube Arrays Subjected to Cross Flow ofWater”.
2. Sandeep R. Desai ,S. Pavitran (2017) : “Experimental Investigation on Vortex Shedding and Fluid Elastic Instability in Finned Tube Arrays Subjected to Water CrossFlow”.
3. Sandeep R Desai and Rohit V Kengar (2019): “Experimental analysis of fluid elastic vibrations in rotated square finned tube arrays subjected to water crossflow”.
4. Sandeep R. Desai and Aslam A. Maniyar (2019): “Fluidelastic Vibration Analysis of Normal Square Finned Tube Arrays in Water Cross Flow”.
5. Sandeep R. Desai<sup>1</sup> ,S. Pavitran<sup>2</sup> : “DESIGN OF FLOW LOOP FLUID ELASTIC VIBRATION EXPERIMENTS”.
6. Pravin h. yadav, dillipkumarmohanty : “ EFFECT OF MATERIAL ON FLUID ELASTIC INSTABILITY OF PARALLEL TRIANGULAR ARRAY SUBJECTED TO WATER CROS”.
7. Jiang Lai, Lei Sun, LixiaGao, Pengzhou Li: “MECHANISM ANALYSIS ON FLUID ELASTIC INSTABILITY OF TUBE BUNDLES IN CONSIDERING OF CROSS-FLOW EFFECTS”.
8. Guillaume Ricciardi, Njuki W. Mureithi and M. J. Pettigrew : “ FLUIDELASTIC INSTABILITY IN A NORMAL TRIANGULAR TUBE BUNDLE SUBJECTED TO AIR-WATER CROSS-FLOW”.
9. Vikram B Yadav, S.R. Desai, M. M. Mirza : “REVIEW ON FLUID-ELASTIC INSTABILITY IN FINNED TUBE ARRAYS”.
10. Hassan Arshad, Luqman Ahmad Nizam, ShahabKhushnood:“EFFECT OF FIN GEOMETRY ON FLOW-INDUCED VIBRATION RESPONSE OF A FINNED TUBE IN A TUBE BUNDLE”.

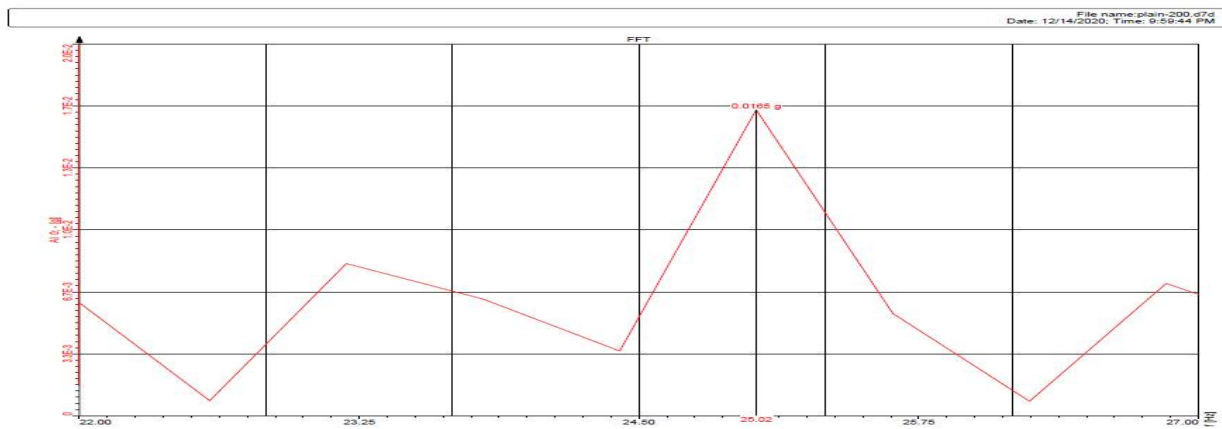
## 9. APPENDICES

Samples of Frequency Spectrum graph as we recorded from 100rpm to 1300rpm during the experimentation for plain tube is as follows.

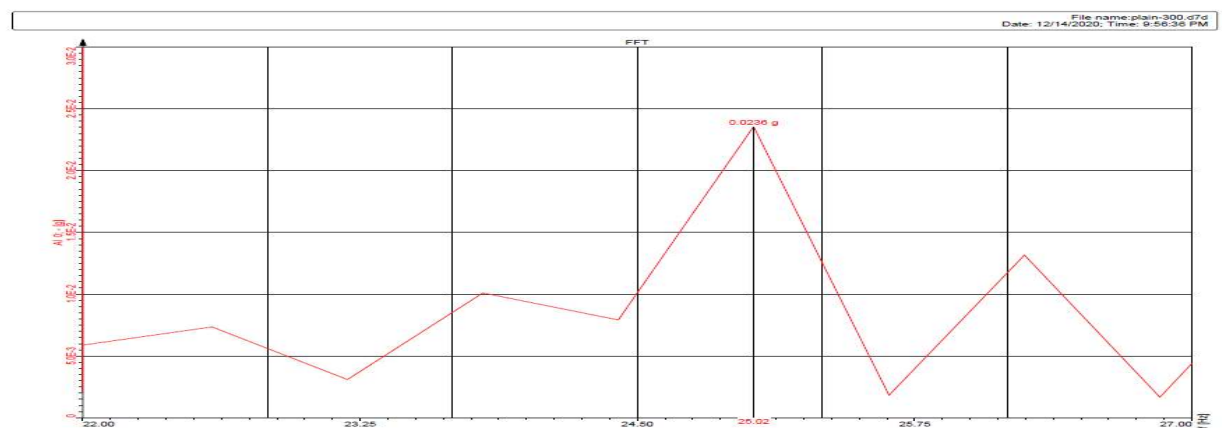
100



200

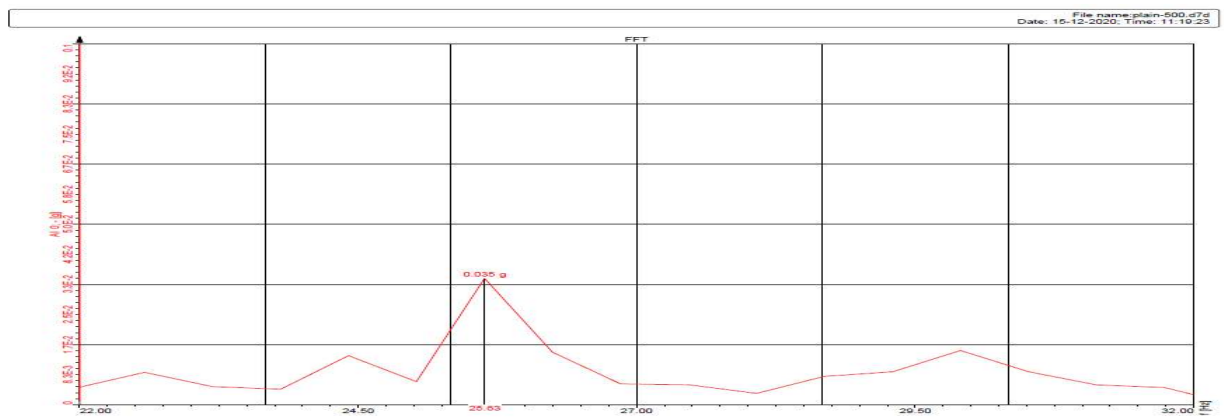


300

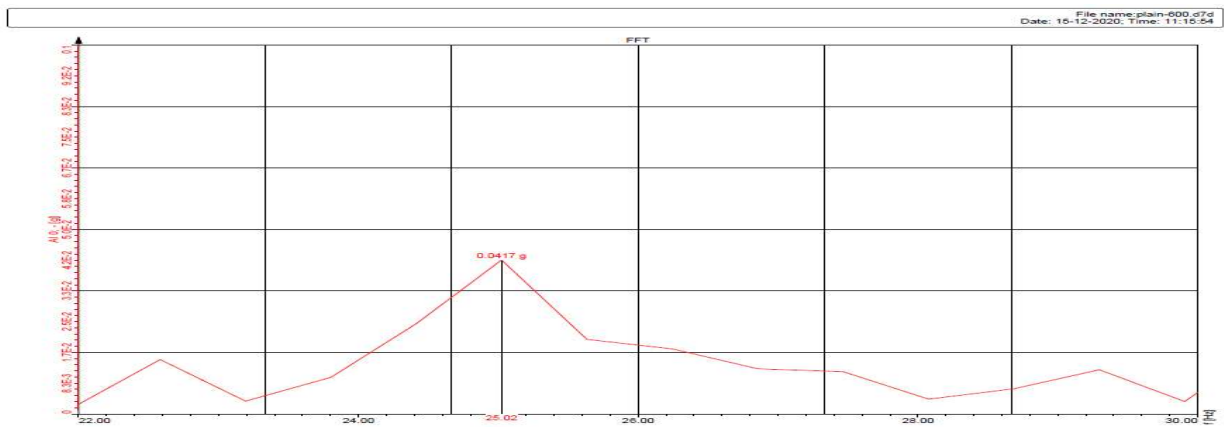




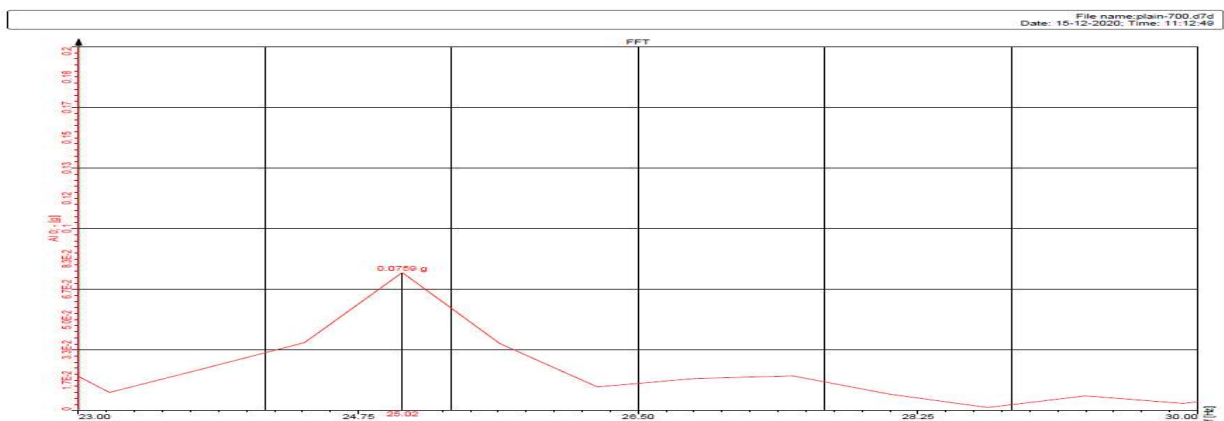
400



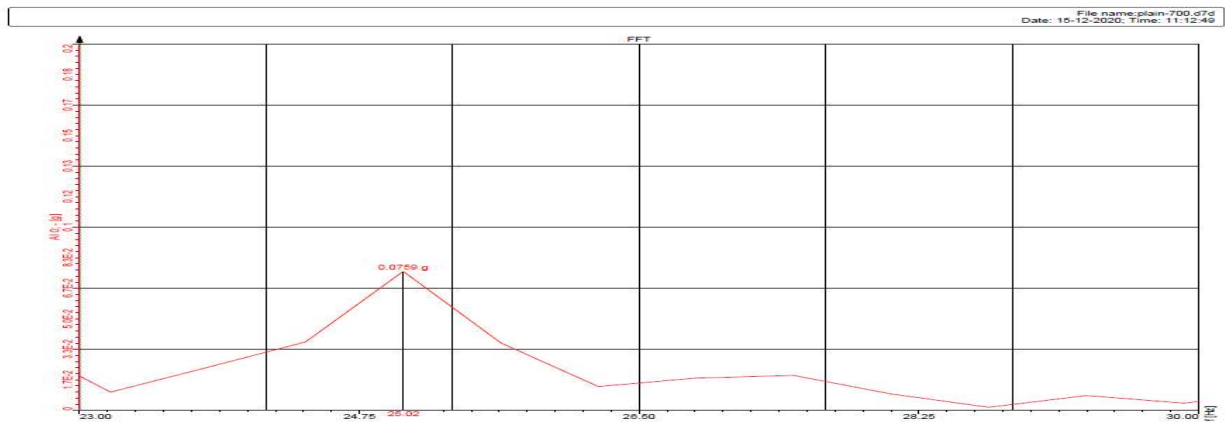
500



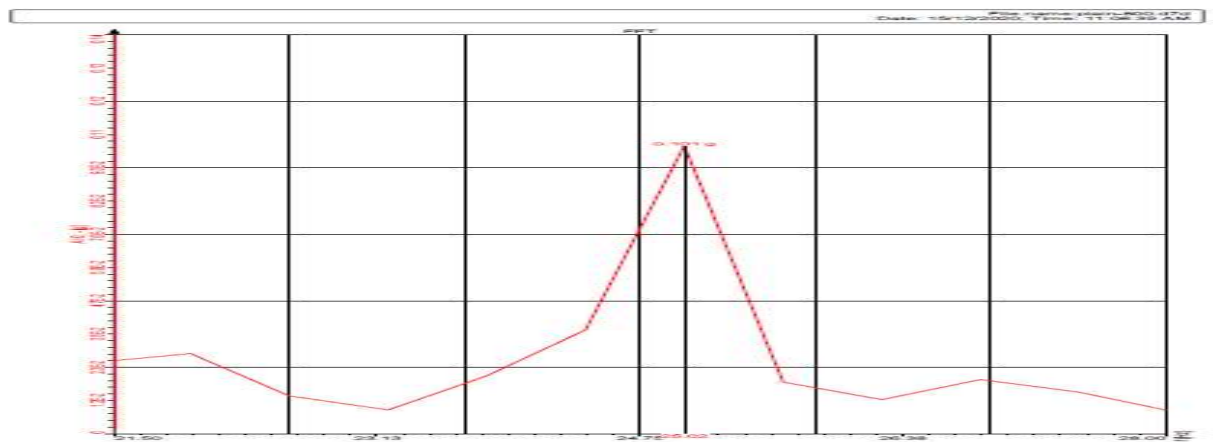
600



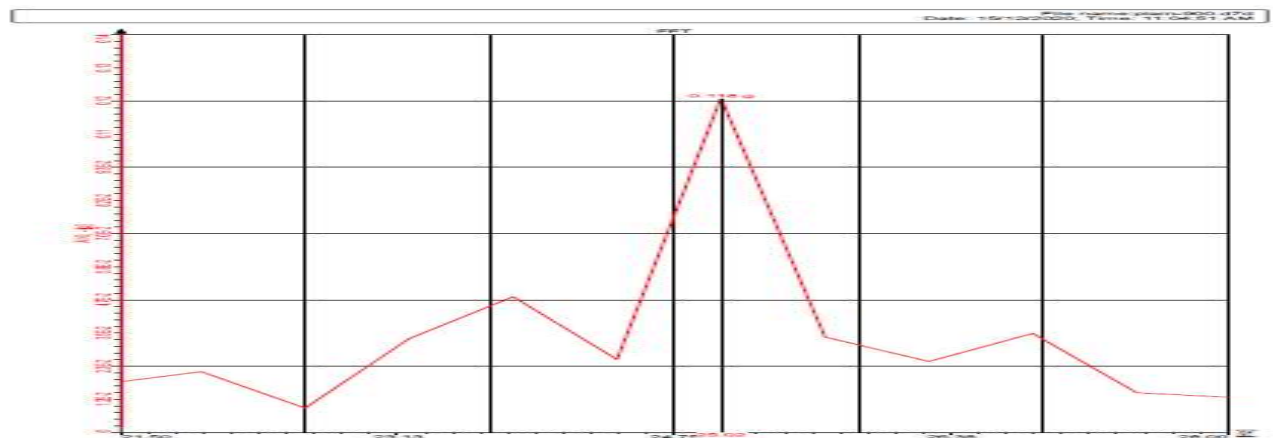
700



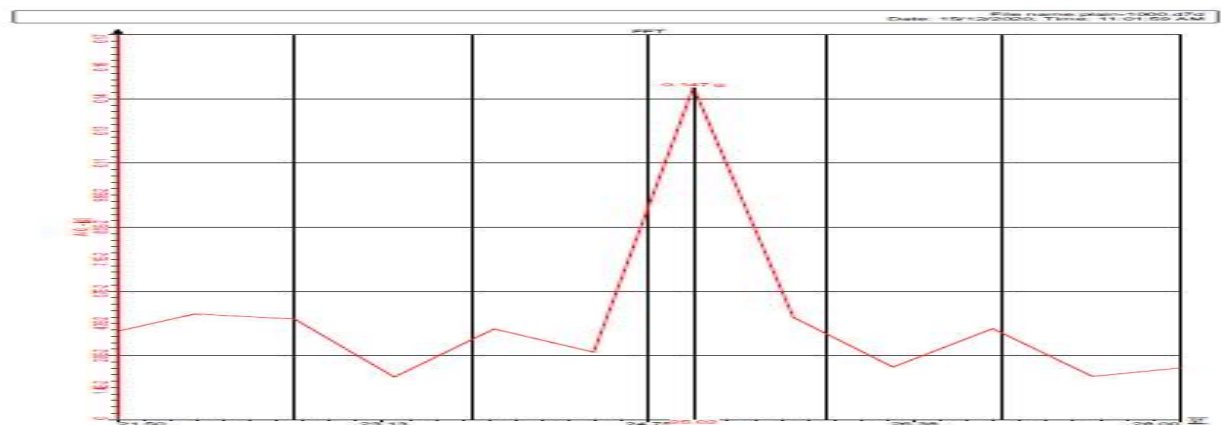
800



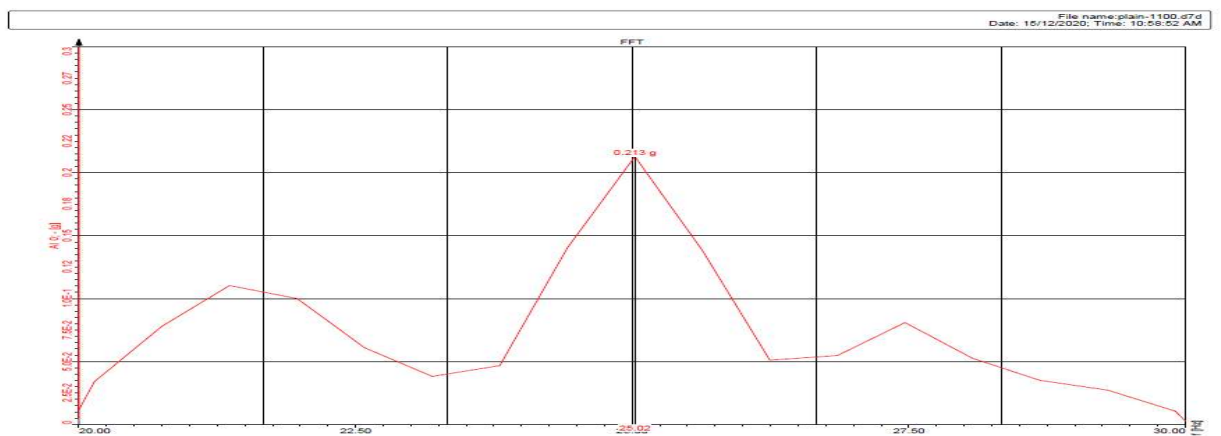
900



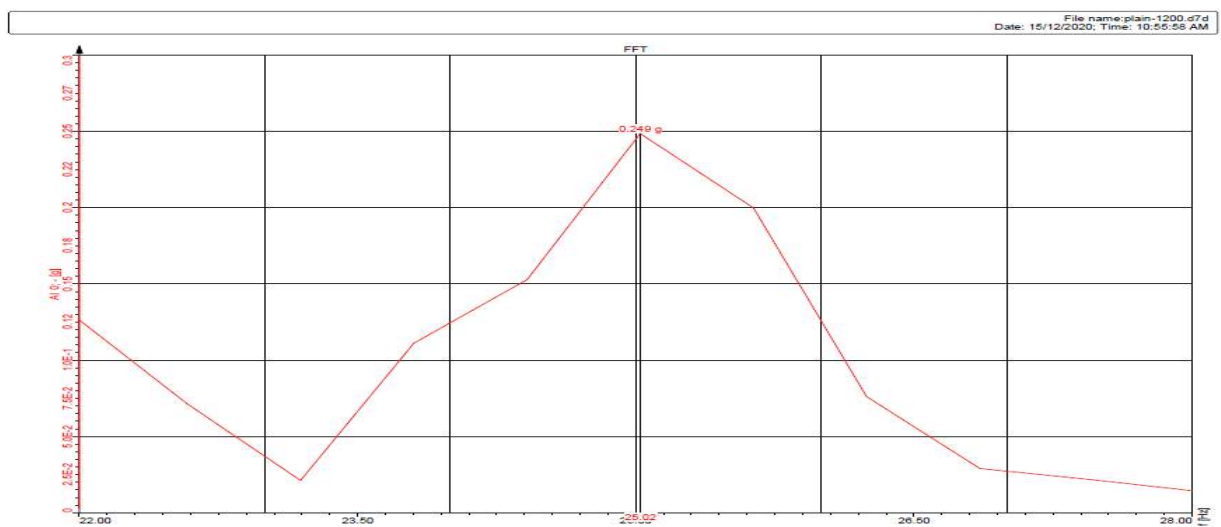
1000



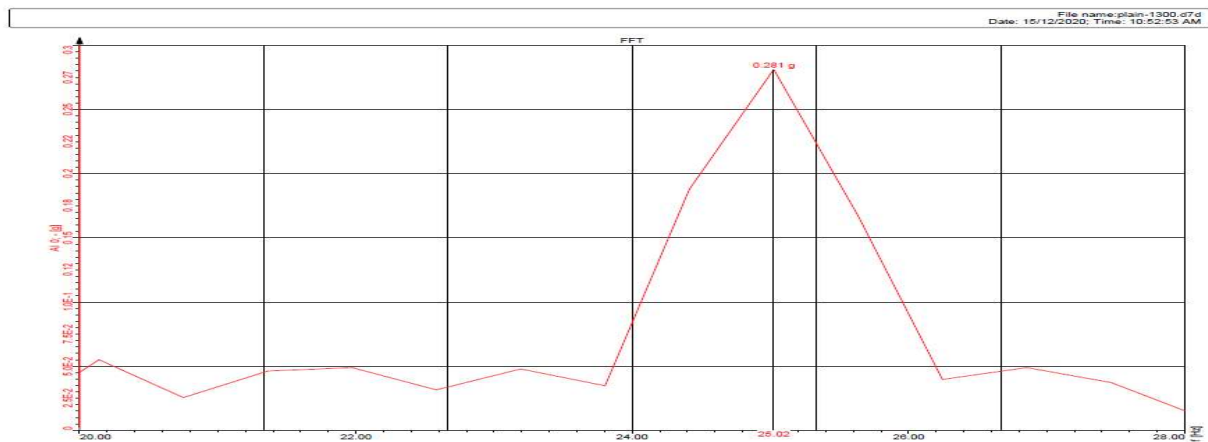
1100



1200



1300



Pictures taken during the experimentation









